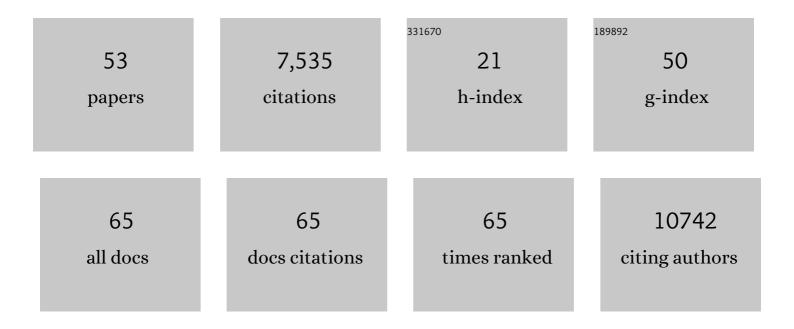
Yao Zhao

List of Publications by Year in descending order

Source: https://exaly.com/author-pdf/3799710/publications.pdf Version: 2024-02-01



#	Article	IF	CITATIONS
1	Structure of Mpro from SARS-CoV-2 and discovery of its inhibitors. Nature, 2020, 582, 289-293.	27.8	3,133
2	Structure of the RNA-dependent RNA polymerase from COVID-19 virus. Science, 2020, 368, 779-782.	12.6	1,228
3	Structure-based design of antiviral drug candidates targeting the SARS-CoV-2 main protease. Science, 2020, 368, 1331-1335.	12.6	1,135
4	Structural basis for the inhibition of SARS-CoV-2 main protease by antineoplastic drug carmofur. Nature Structural and Molecular Biology, 2020, 27, 529-532.	8.2	339
5	Advances in Toxicological Research of the Anticancer Drug Cisplatin. Chemical Research in Toxicology, 2019, 32, 1469-1486.	3.3	215
6	Crystal Structures of Membrane Transporter MmpL3, an Anti-TB Drug Target. Cell, 2019, 176, 636-648.e13.	28.9	172
7	Inhibition mechanism of SARS-CoV-2 main protease by ebselen and its derivatives. Nature Communications, 2021, 12, 3061.	12.8	149
8	Crystal structure of SARS-CoV-2 main protease in complex with protease inhibitor PF-07321332. Protein and Cell, 2022, 13, 689-693.	11.0	136
9	Breaking the Intracellular Redox Balance with Diselenium Nanoparticles for Maximizing Chemotherapy Efficacy on Patient-Derived Xenograft Models. ACS Nano, 2020, 14, 16984-16996.	14.6	105
10	High-throughput screening identifies established drugs as SARS-CoV-2 PLpro inhibitors. Protein and Cell, 2021, 12, 877-888.	11.0	95
11	Structures of cell wall arabinosyltransferases with the anti-tuberculosis drug ethambutol. Science, 2020, 368, 1211-1219.	12.6	82
12	A Near-Infrared-II Polymer with Tandem Fluorophores Demonstrates Superior Biodegradability for Simultaneous Drug Tracking and Treatment Efficacy Feedback. ACS Nano, 2021, 15, 5428-5438.	14.6	79
13	Structural basis for replicase polyprotein cleavage and substrate specificity of main protease from SARS-CoV-2. Proceedings of the National Academy of Sciences of the United States of America, 2022, 119, e2117142119.	7.1	64
14	Uptake and Transformation of Silver Nanoparticles and Ions by Rice Plants Revealed by Dual Stable Isotope Tracing. Environmental Science & Technology, 2019, 53, 625-633.	10.0	52
15	The gut microbiota in larvae of the housefly Musca domestica and their horizontal transfer through feeding. AMB Express, 2017, 7, 147.	3.0	49
16	Bacterial communities of the cotton aphid Aphis gossypii associated with Bt cotton in northern China. Scientific Reports, 2016, 6, 22958.	3.3	46
17	Potential-Dynamic Surface Chemistry Controls the Electrocatalytic Processes of Ethanol Oxidation on Gold Surfaces. ACS Energy Letters, 2019, 4, 215-221.	17.4	45
18	A negatively charged Pt(<scp>iv</scp>) prodrug for electrostatic complexation with polymers to overcome cisplatin resistance. Journal of Materials Chemistry B, 2019, 7, 3346-3350.	5.8	27

ΥΑΟ ΖΗΑΟ

#	Article	IF	CITATIONS
19	In Situ Liquid Secondary Ion Mass Spectrometry: A Surprisingly Soft Ionization Process for Investigation of Halide Ion Hydration. Analytical Chemistry, 2019, 91, 7039-7046.	6.5	27
20	Structural insights into substrate recognition by the type VII secretion system. Protein and Cell, 2020, 11, 124-137.	11.0	25
21	Bt proteins Cry1Ah and Cry2Ab do not affect cotton aphid Aphis gossypii and ladybeetle Propylea japonica. Scientific Reports, 2016, 6, 20368.	3.3	24
22	A Photoactive Platinum(IV) Anticancer Complex Inhibits Thioredoxin–Thioredoxin Reductase System Activity by Induced Oxidization of the Protein. Inorganic Chemistry, 2018, 57, 5575-5584.	4.0	24
23	Impact of Single and Stacked Insect-Resistant Bt-Cotton on the Honey Bee and Silkworm. PLoS ONE, 2013, 8, e72988.	2.5	24
24	Identification of proteasome and caspase inhibitors targeting SARS-CoV-2 Mpro. Signal Transduction and Targeted Therapy, 2021, 6, 214.	17.1	17
25	Tea saponin reduces the damage of <i> Ectropis obliqua</i> to tea crops, and exerts reduced effects on the spiders <i>Ebrechtella tricuspidata</i> and <i> Evarcha albaria</i> compared to chemical insecticides. PeerJ, 2018, 6, e4534.	2.0	15
26	Proteomic Strategy for Identification of Proteins Responding to Cisplatin-Damaged DNA. Analytical Chemistry, 2019, 91, 6035-6042.	6.5	14
27	Cryo-EM snapshots of mycobacterial arabinosyltransferase complex EmbB2-AcpM2. Protein and Cell, 2020, 11, 505-517.	11.0	13
28	Hydrogen Isotope Effects on Aqueous Electrolyte for Electrochemical Lithiumâ€lon Storage. Angewandte Chemie - International Edition, 2022, 61, .	13.8	13
29	Real-Time Characterization of the Fine Structure and Dynamics of an Electrical Double Layer at Electrode–Electrolyte Interfaces. Journal of Physical Chemistry Letters, 2021, 12, 5279-5285.	4.6	12
30	<i>In Situ</i> Visualization of Proteins in Single Cells by Time-of-Flight–Secondary Ion Mass Spectrometry Coupled with Genetically Encoded Chemical Tags. Analytical Chemistry, 2020, 92, 15517-15525.	6.5	11
31	Photo-induced mitochondrial DNA damage and NADH depletion by –NO ₂ modified Ru(<scp>ii</scp>) complexes. Chemical Communications, 2021, 57, 4162-4165.	4.1	11
32	Unexpected Thymine Oxidation and Collision-Induced Thymine-Pt-guanine Cross-Linking on 5′-TpG and 5′-GpT by a Photoactivatable Diazido Pt(IV) Anticancer Complex. Inorganic Chemistry, 2020, 59, 8468-8480.	4.0	10
33	Cisplatinâ€induced alteration on membrane composition of A549 cells revealed by ToFâ€SIMS. Surface and Interface Analysis, 2020, 52, 256-263.	1.8	9
34	Solvent-dependent structural dynamics of an azido-platinum complex revealed by linear and nonlinear infrared spectroscopy. Physical Chemistry Chemical Physics, 2018, 20, 9984-9996.	2.8	8
35	Organometallic ruthenium anticancer complexes inhibit human peroxiredoxin I activity by binding to and inducing oxidation of its catalytic cysteine residue. Metallomics, 2019, 11, 546-555.	2.4	8
36	Atmospheric particulate characterization by ToF-SIMS in an urban site in Beijing. Atmospheric Environment, 2020, 220, 117090.	4.1	8

ΥΑΟ ΖΗΑΟ

#	Article	IF	CITATIONS
37	Photoactivatable diazido Pt(iv) anticancer complex can bind to and oxidize all four nucleosides. Dalton Transactions, 2020, 49, 17157-17163.	3.3	7
38	Reactions of a photoactivatable diazido Pt(iv) anticancer complex with a single-stranded oligodeoxynucleotide. Dalton Transactions, 2020, 49, 11249-11259.	3.3	7
39	Biodiversity Survey of Flower-Visiting Spiders Based on Literature Review and Field Study. Environmental Entomology, 2020, 49, 673-682.	1.4	7
40	Tandem Mass Spectrometry Reveals Preferential Ruthenation of Thymines in Human Telomeric G-Quadruplex DNA by an Organometallic Ruthenium Anticancer Complex. Organometallics, 2020, 39, 3315-3322.	2.3	6
41	G-quadruplex inducer/stabilizer pyridostatin targets <i>SUB1</i> to promote cytotoxicity of a transplatinum complex. Nucleic Acids Research, 2022, 50, 3070-3082.	14.5	6
42	Scaled conductance quantization unravels the switching mechanism in organic ternary resistive memories. Journal of Materials Chemistry C, 2020, 8, 2964-2969.	5.5	5
43	Heterogeneous Reaction of HCOOH on NaCl Particles at Different Relative Humidities. Journal of Physical Chemistry A, 2018, 122, 7218-7226.	2.5	3
44	Mass spectrometric quantification of the binding ratio of metalâ€based anticancer complexes with protein thiols. Rapid Communications in Mass Spectrometry, 2019, 33, 951-958.	1.5	3
45	ToFâ€SIMS analysis of chemical composition of atmospheric aerosols in Beijing. Surface and Interface Analysis, 2020, 52, 272-282.	1.8	3
46	Hydrogen Isotope Effects on Aqueous Electrolyte for Electrochemical Lithiumâ€ l on Storage. Angewandte Chemie, 0, , .	2.0	3
47	Snapshots of catalysis: Structure of covalently bound substrate trapped in Mycobacterium tuberculosis thiazole synthase (ThiG). Biochemical and Biophysical Research Communications, 2018, 497, 214-219.	2.1	2
48	Transcriptome responses to elevated CO 2 level and Wolbachia â€infection stress in Hylyphantes graminicola (Araneae: Linyphiidae). Insect Science, 2020, 27, 908-920.	3.0	1
49	Open-flow microperfusion combined with mass spectrometry for <i>in vivo</i> liver lipidomic analysis. Analyst, The, 2021, 146, 1915-1923.	3.5	1
50	ToF-SIMS characterization of surface chemical evolution on electrode surfaces educed by electrochemical activation. Journal of Analytical Atomic Spectrometry, 2022, 37, 890-897.	3.0	1
51	Modest sexual size dimorphism and allometric growth: a study based on growth and gonad development in the wolf spider <i>Pardosa pseudoannulata</i> (Araneae: Lycosidae). Biology Open, 2021, 10, .	1.2	1
52	Elevated CO2 concentration affects survival, but not development, reproduction, or predation of the predator Hylyphantes graminicola (Araneae: Linyphiidae). Environmental Pollution, 2021, 288, 117791.	7.5	0
53	Serum phosphopeptide profiling for colorectal cancer diagnosis using liquid chromatography–mass spectrometry. Rapid Communications in Mass Spectrometry, 2022, 36, e9316.	1.5	0